*Exceptional service in the national interest*

SAND2016-9996C

Sandia National Laboratories

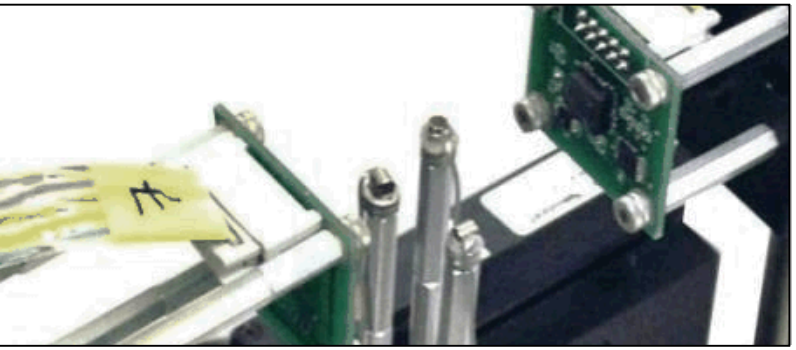

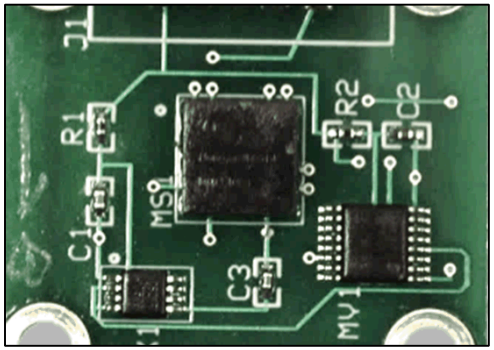


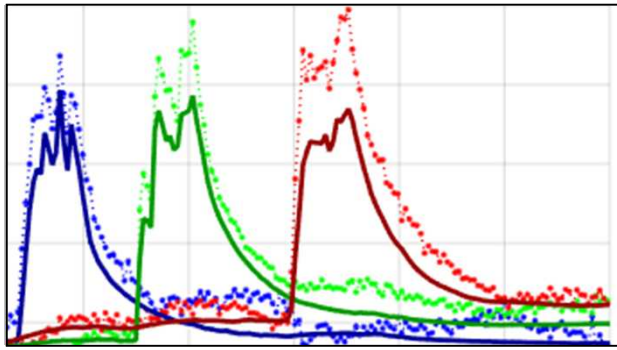

# Wireless Temperature Sensing Using Permanent Magnets for Multiple Points Undergoing Repeatable Motions

Yi Chen*, Oksana Guba, Carlton F. Brooks, Christine C. Roberts,
Bart G. van Bloemen Waanders and Martin B. Nemer

ASME Dynamic Systems and Control Conference
In Minneapolis, Minnesota on Wednesday, October 12th, 2016
18-1 Sensors and Actuators
DSCC2016-9663

Sandia National Laboratories, P.O. Box 5800
Albuquerque, NM 87185, USA
*yichen@sandia.gov

U.S. DEPARTMENT OF ENERGY

NNSA National Nuclear Security Administration

Sandia National Laboratories is a multi-program laboratory managed and operated by Sandia Corporation, a wholly owned subsidiary of Lockheed Martin Corporation, for the U.S. Department of Energy's National Nuclear Security Administration under contract DE-AC04-94AL85000. SAND NO. 2011-XXXXP

# Motivation

- **Problem:** Many applications require **compact** temperature sensors with **no wire feedthroughs**, **no optical access**, and **no extra power systems** at **multiple sensing points**
- **Proposed Solution:** Magnetic temperature sensing

## Sealed Opaque Vessels

### Pressure Vessels

© Parr Instrument Company

### Batteries


© Fusion AGM Batteries

### Foam Molds

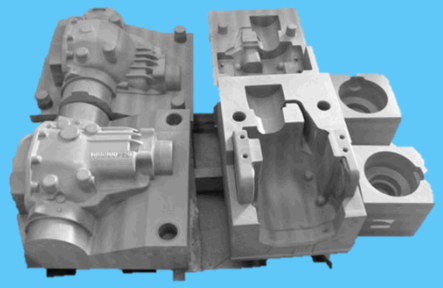

© Pembuatan Pola Untuk Casting

## Objects under Motions

### Rotating Bearing

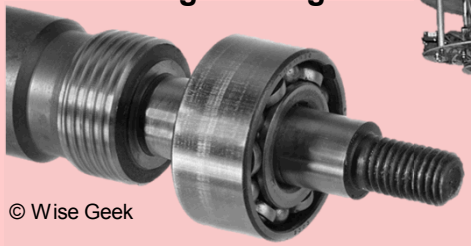

© Wise Geek

### Complex Manipulators

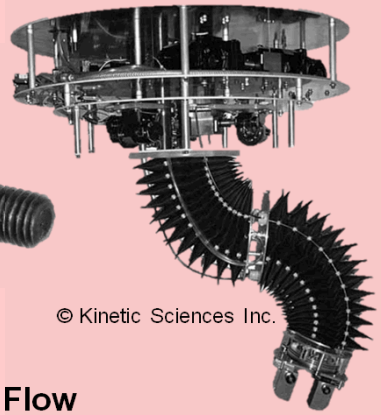

© Kinetic Sciences Inc.

### Particles in a Flow

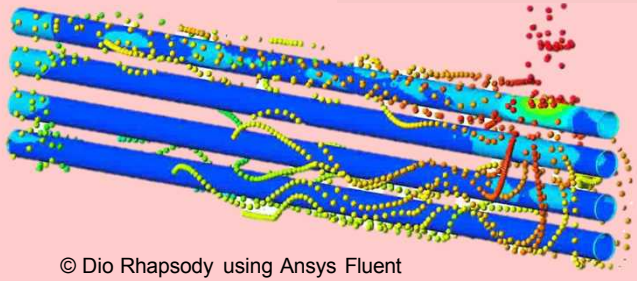

© Dio Rhapsody using Ansys Fluent

Reproduced for educational purposes only under fair use.

# Concept

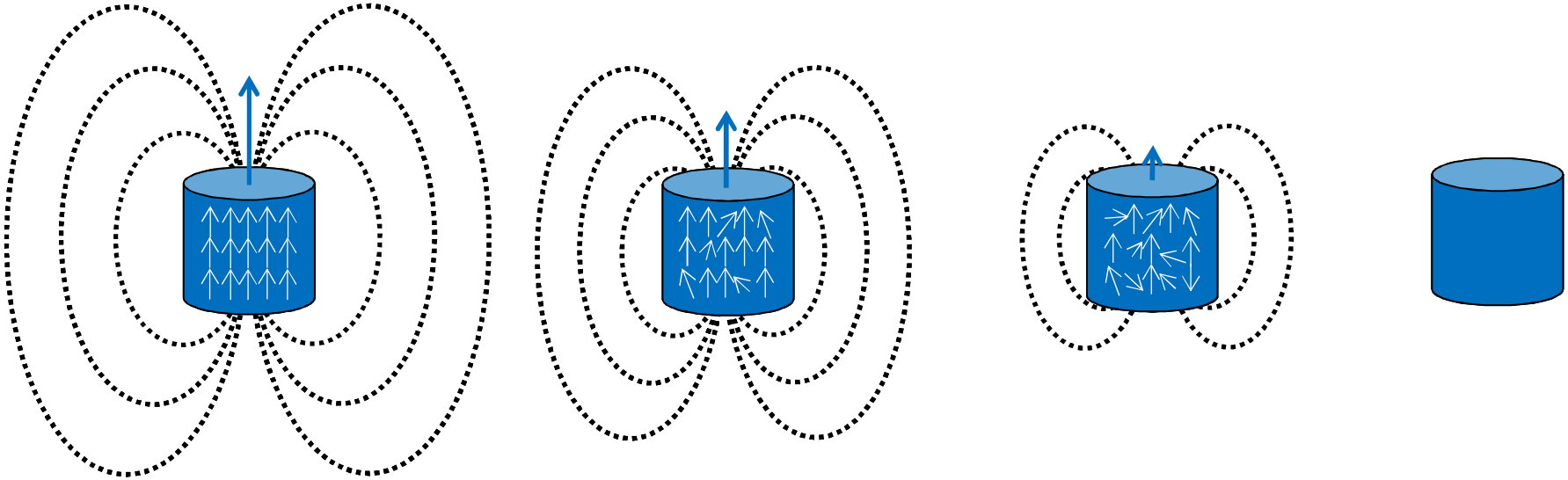


**Prior art measured temperature using a single magnet or as a bulk average:**

- Temperature sensing by measuring the magnetic field loss in permanent magnet motors (Regiosa et al. 2012)
- Temperature sensing with a single fixed magnet (Gupta and Peroulis 2012)

# Temperature of Multiple Magnets

Sandia National Laboratories

**Model**

- The magnetic field of each magnet sums linearly
- Cylinder magnets behaves similar to a dipole model

$$\mathbf{B}_i = \sum_{j=1}^{J} B_{Tj}(T_j)\left(\frac{3(\mathbf{H}_j \cdot \mathbf{X}_{ij})\mathbf{X}_{ij}}{R_{ij}^5} - \frac{\mathbf{H}_j}{R_{ij}^3}\right)$$

$$\mathbf{B}_i = B_{ix}\hat{\mathbf{x}} + B_{iy}\hat{\mathbf{y}} + B_{iz}\hat{\mathbf{z}}$$

- We are operating in the linear recoverable region and the field magnitude is isotropic with temperature

$$B_{Tj}(T_j) = B_T(T_0)\left[1 - C_T(T_j - T_0)\right]$$

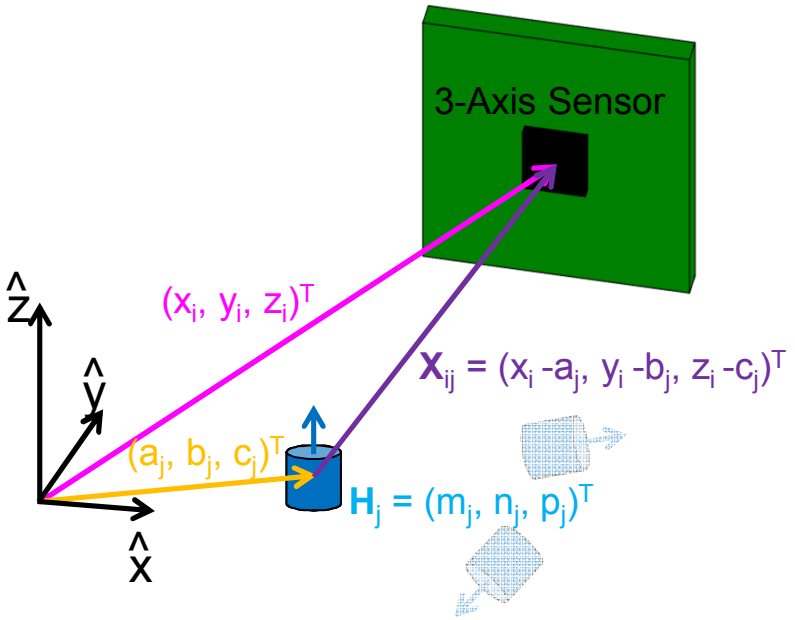


Calibrating for $C_T$ in a N52 Nd-Fe-B Magnet

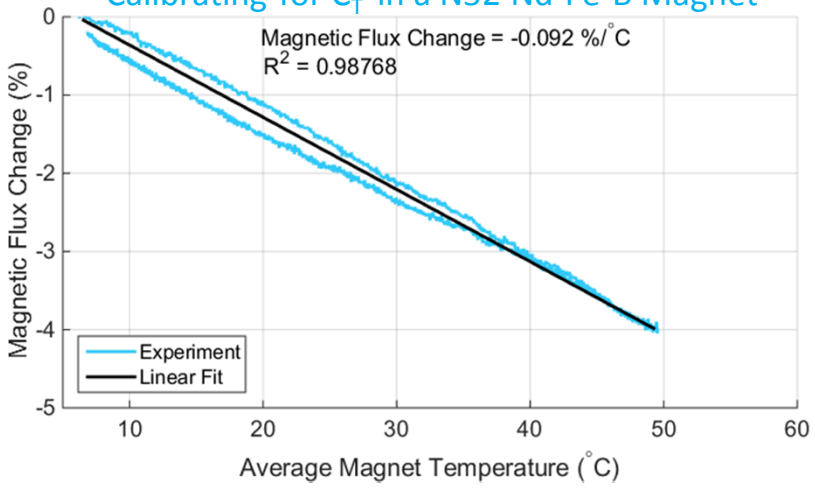


Dipole Model field vs. Measured field

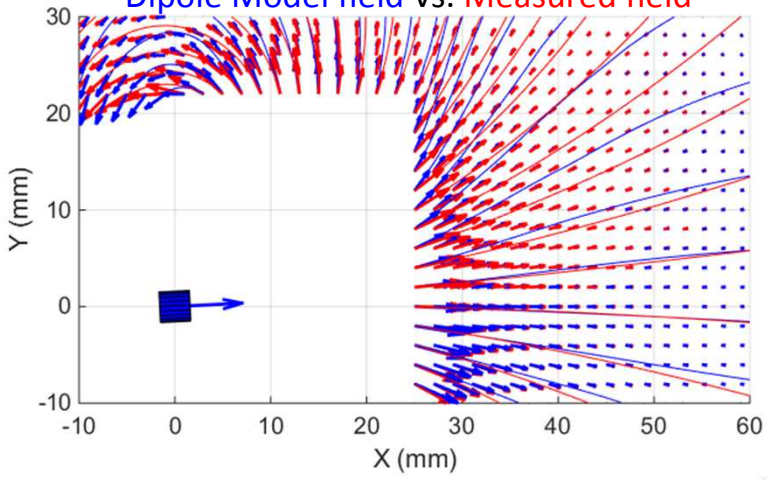

# Temperature of Multiple Magnets

Sandia National Laboratories

**Model**

- The magnetic field of each magnet sums linearly
- Cylinder magnets behaves similar to a dipole model

$$\mathbf{B}_i = \sum_{j=1}^{J} B_{Tj}(T_j)\left(\frac{3(\mathbf{H}_j \cdot \mathbf{X}_{ij})\mathbf{X}_{ij}}{R_{ij}^5} - \frac{\mathbf{H}_j}{R_{ij}^3}\right)$$

$$\mathbf{B}_i = B_{ix}\hat{\mathbf{x}} + B_{iy}\hat{\mathbf{y}} + B_{iz}\hat{\mathbf{z}}$$

- We are operating in the linear recoverable region and the field magnitude is isotropic with temperature

$$B_{Tj}(T_j) = B_T(T_0)\left[1 - C_T(T_j - T_0)\right]$$

**Solution**

- Assume position and orientation fixed, known, or can be calibrated via a variety of methods, then the only unknown is $T_j$ in $B_{Tj}(T_j)$. The system becomes **linear**.
- With J magnets and I magnetic sensor axes (I ≥ J), we can rewrite in matrix form

$$\mathbf{Y} = \mathbf{P}\,\mathbf{A}$$

- With the least squares solution

$$\mathbf{A} = (\mathbf{P}^T\mathbf{P})^{-1}\mathbf{P}^T\mathbf{Y} \quad \text{such that} \quad T_j = \frac{1}{C_T}(1 - A_j) + T_0$$

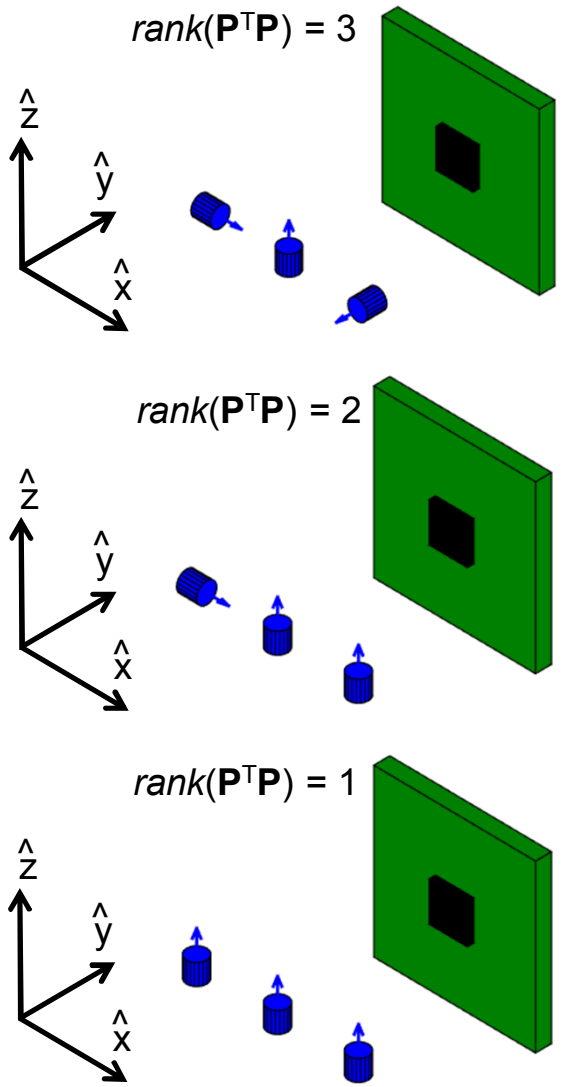

# Experimental Setup

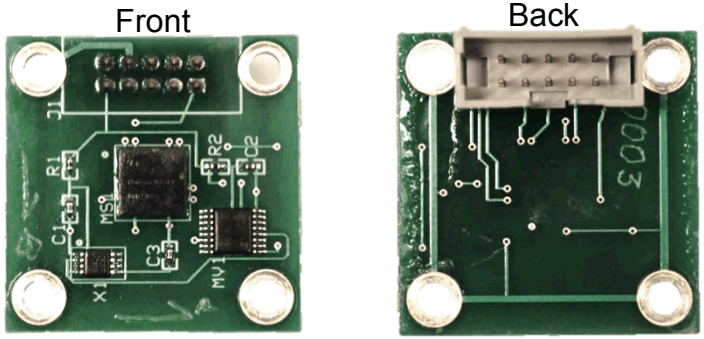


- Custom boards for HMC 1053 magnetoresistive 3-Axis Magnetic Field Sensors
  - NI 16-Bit Analog PXI6255 cards
  - ±6 Gauss with max resolution of 120 µG (DAQ limits resolution to 600 µG)
  - Calibrated with Helmholtz coil and NIST traceable gaussmeter
- Two CMA-25CCCL linear stages
- 3.175 mm N52 cylindrical magnets
- Aluminum and non-magnetic mounting components
- Temperature sources are hot and cold water
- Type K thermocouples for reference (not perfect temperature match due to contact resistance)
- Labview User Interface (sampled 0.28 Hz)

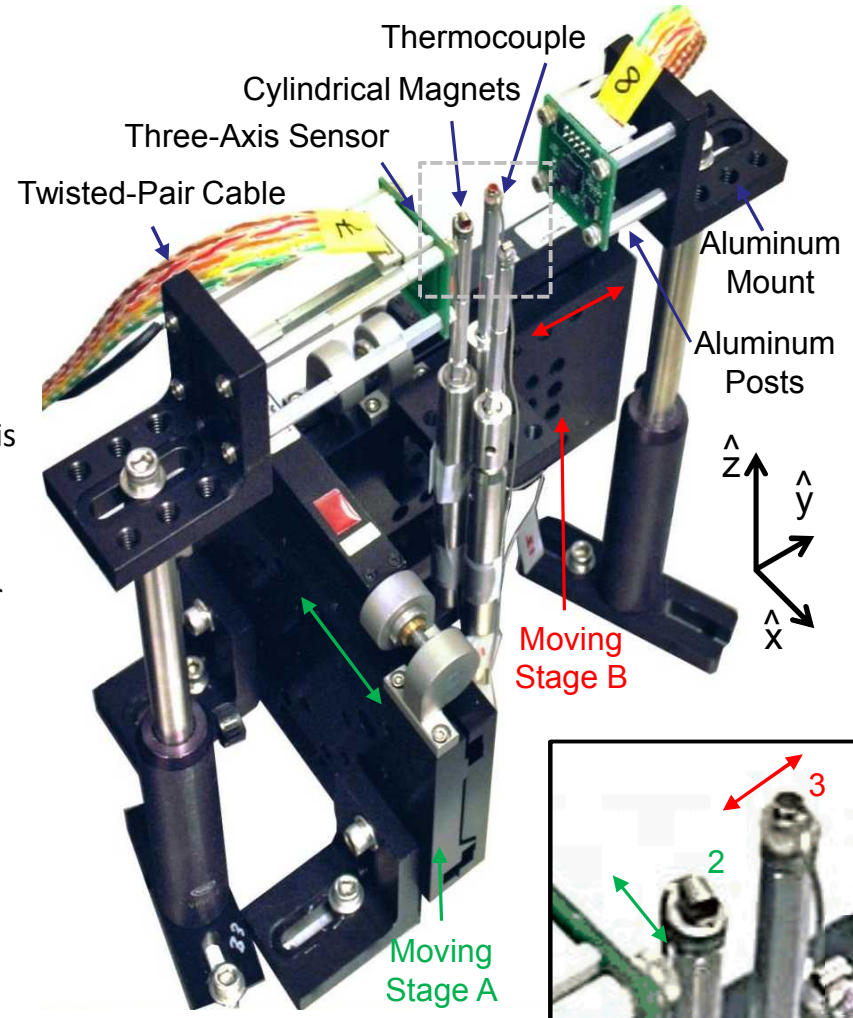

# Stationary Magnets

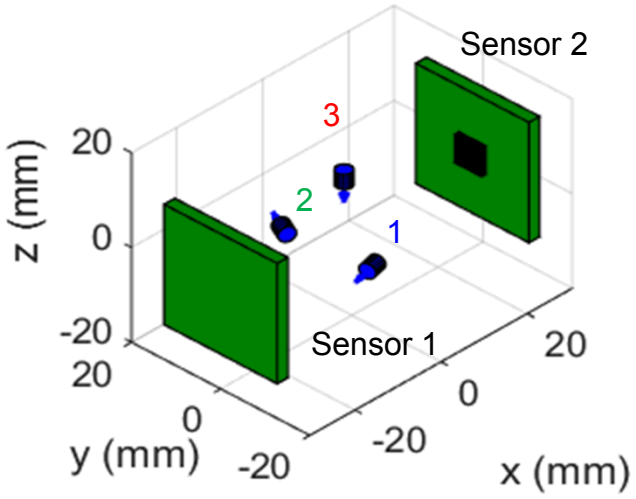


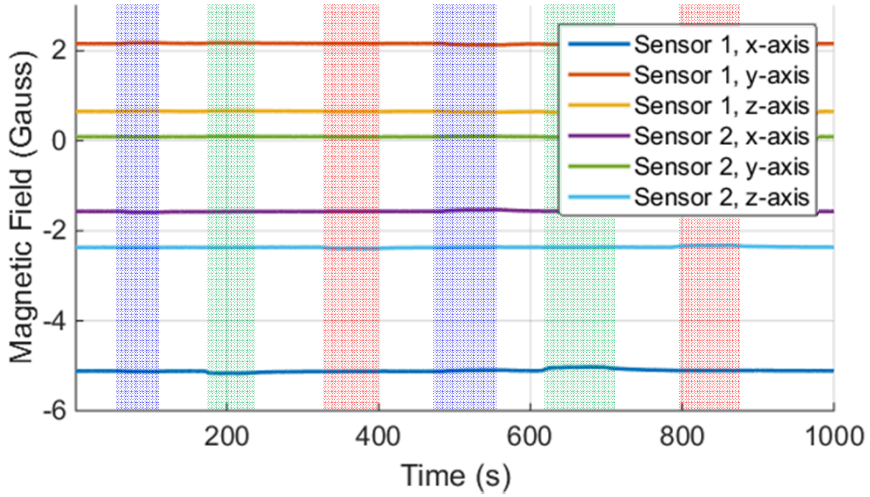


- Two sensors (I = 6) and 3 magnets (J = 3)
- Applied cold water to each magnet in sequence followed by hot water in sequence
- The measured change in the field is small because $C_T$ is small
- When the temperature is solved, the cold and hot source responses can be seen and match with the thermocouple measurements

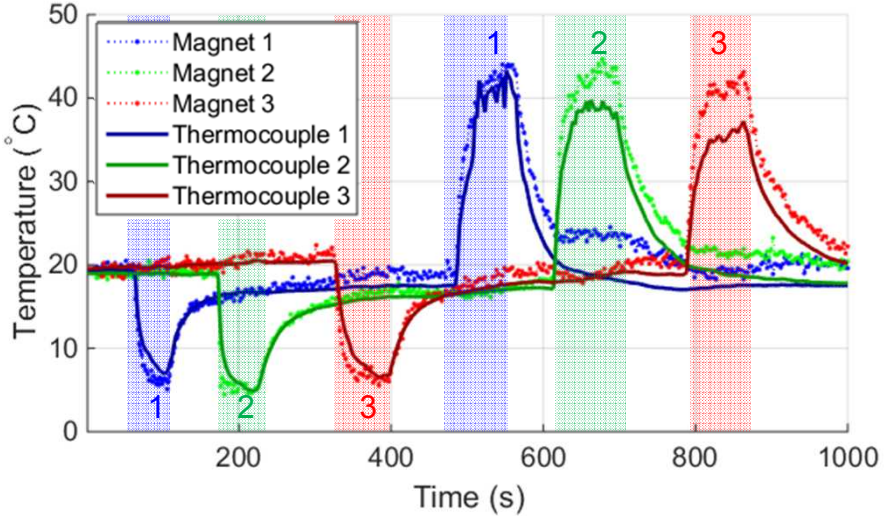

# Moving Magnets: Untracked Positions

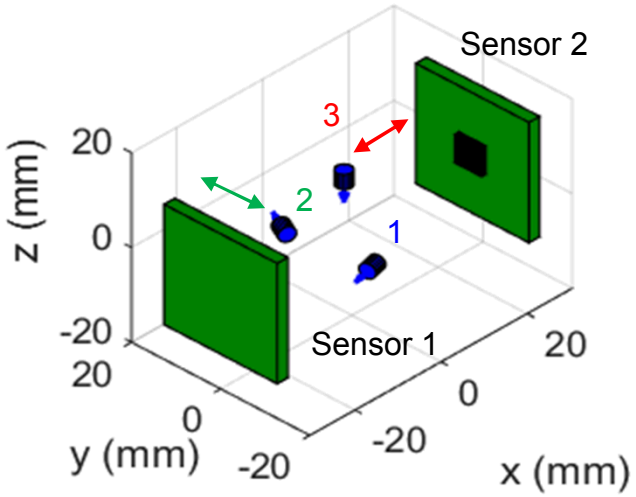


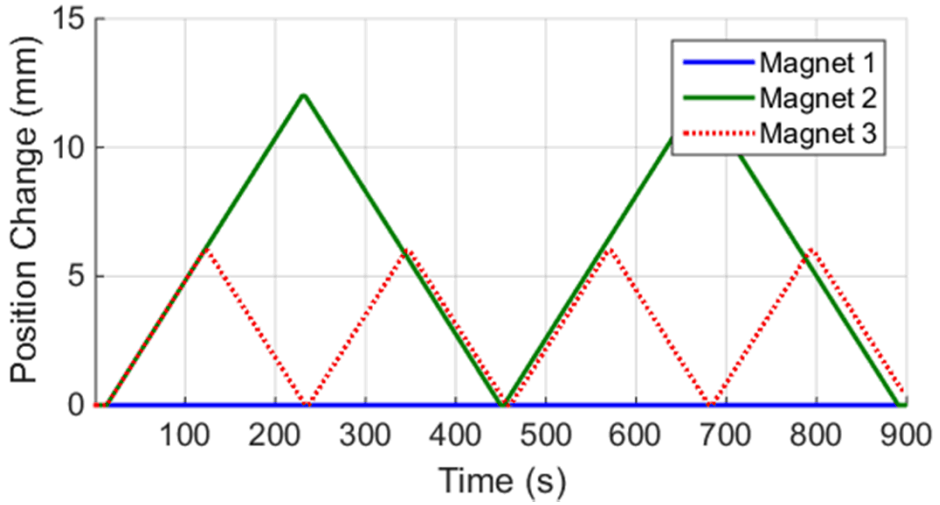


- Moving the magnets
  - Magnet 1 stationary
  - Magnet 2 moves up to 12 mm in 0.2 mm steps
  - Magnet 3 moves up to 6 mm in 0.2 mm steps
- The magnet movement dominates the field measurement
- If the position is untracked or unknown, the temperature estimate is wrong

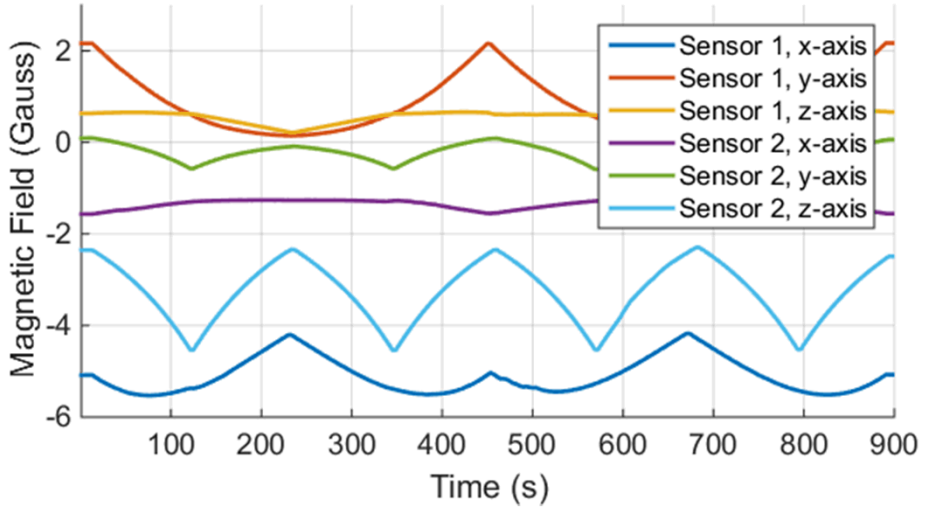

# Moving Magnets: Untracked Positions

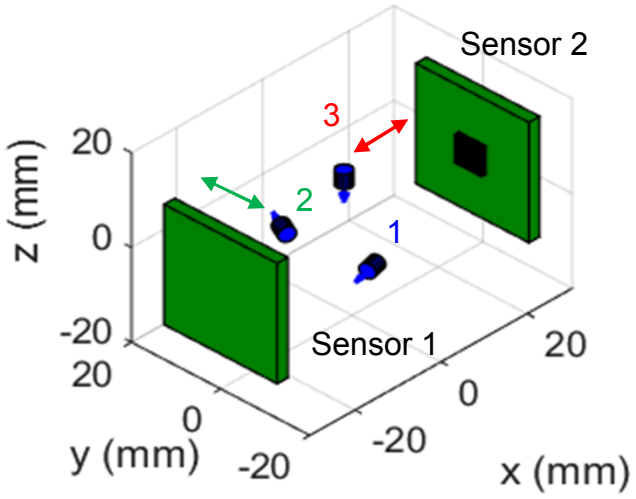


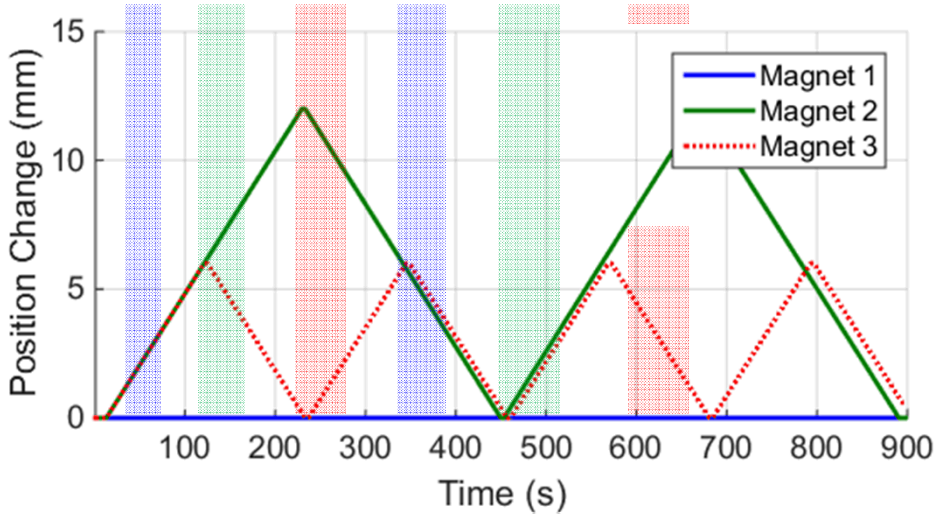


- Moving the magnets
  - Magnet 1 stationary
  - Magnet 2 moves up to 12 mm in 0.2 mm steps
  - Magnet 3 moves up to 6 mm in 0.2 mm steps
- The magnet movement dominates the field measurement
- If the position is untracked or unknown, the temperature estimate is wrong

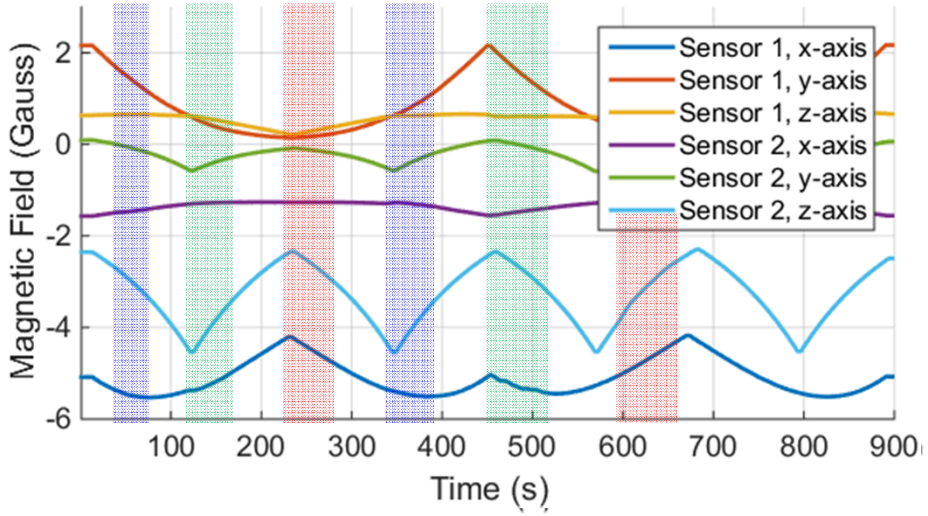

# Moving Magnets: Tracked Positions

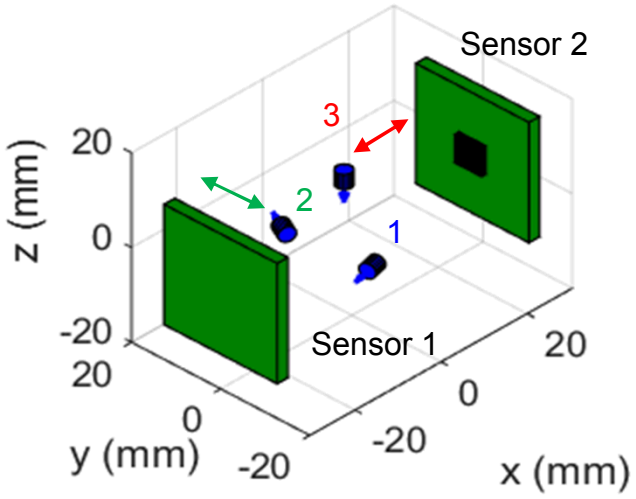


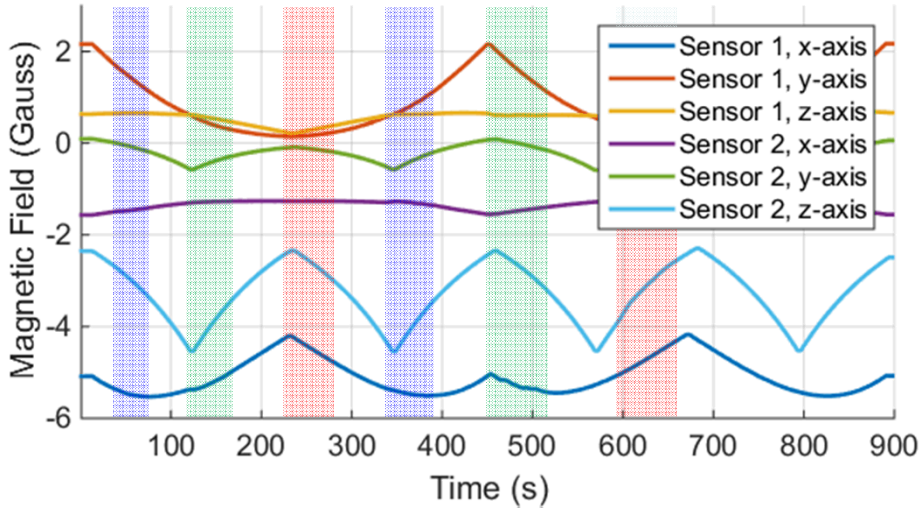


- Create calibrations of the **P** matrix terms at each position of each magnet
- Calibrations of each combination of magnets is not needed since the system is linear
- Using the new **P** matrix calibrations to solve for temperature and we can recover the applied temperatures well

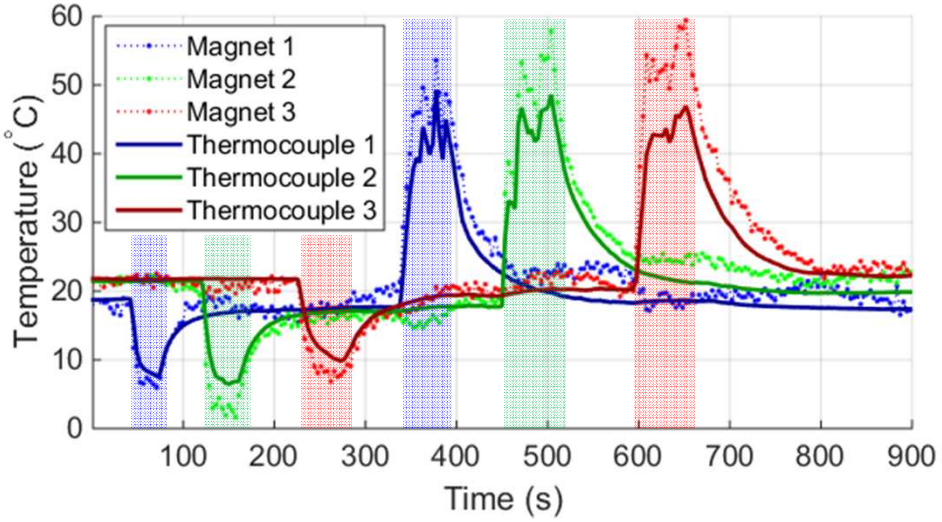

# Moving Magnets: Error Estimation

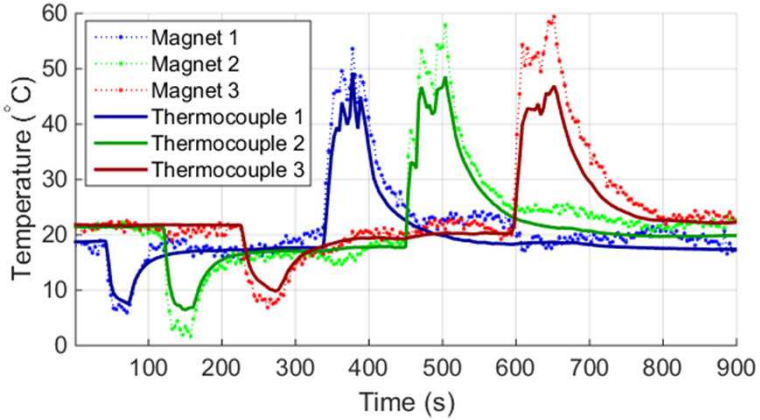


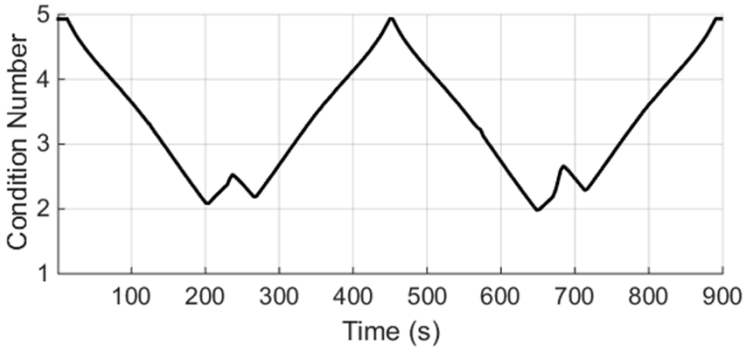


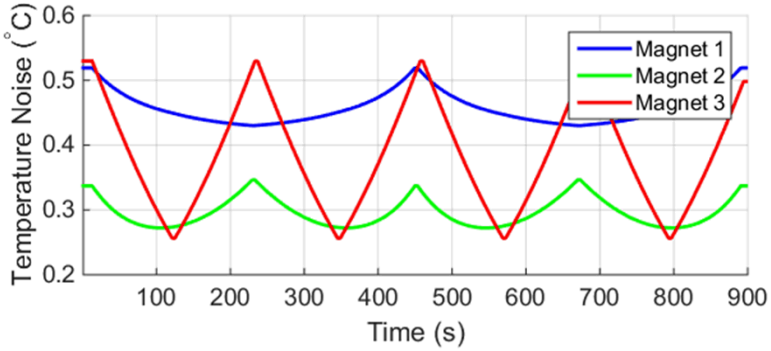


- For 2 sensors (I=6) and three magnets (J =3)
- We can evaluate the **P** matrix condition number at every point in time
- We can also evaluate the estimation noise which comes from
  - Electronic sensor noise (standard deviation)
  - Covariance Matrix

$$\hat{\epsilon}_{Tj} \approx \frac{\epsilon_B}{C_T}\sqrt{diag\left((\mathbf{P}^\intercal\mathbf{P})^{-1}\right)_j}$$

- For this configuration, the condition number is low near 5
- The temperature noise estimate is on the order of 0.5 degrees C varying with position changes of the magnets.

# Moving Magnets: Error Estimation

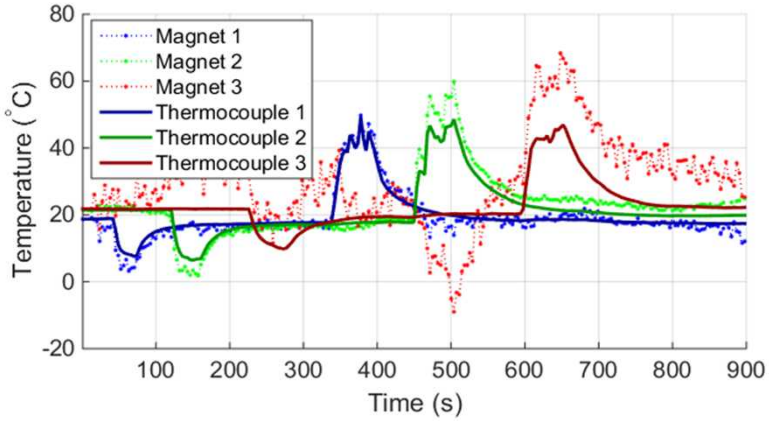


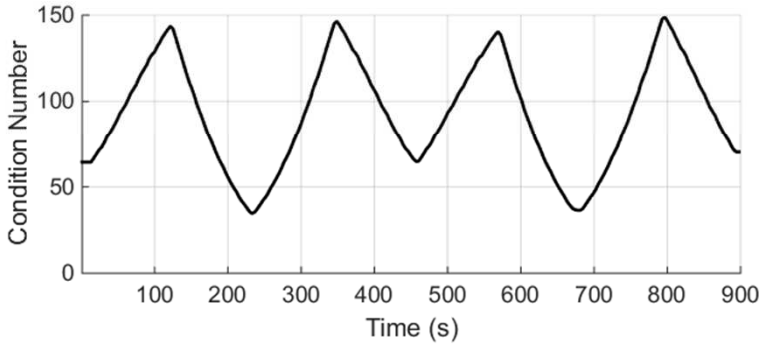


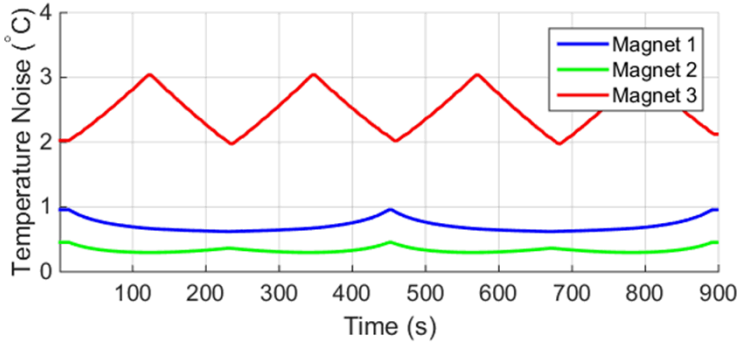


- For the same experiment removing the data from one of the sensors completely gives 1 sensor (I = 3) and three magnets (J = 3) for a square **P** matrix
- The condition number increases drastically to as high as 150
- The temperature noise increases drastically up to 3 degrees C
- Careful selection of magnet orientations, sensor positions and the quantity of magnets and sensors is required to obtain low-noise temperature solutions

# Conclusions and Future Work

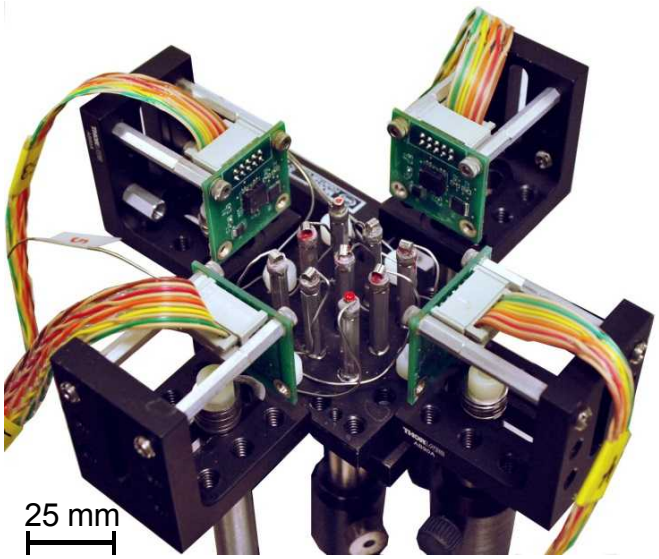


Sensing temperature of array of 9 magnets simultaneously

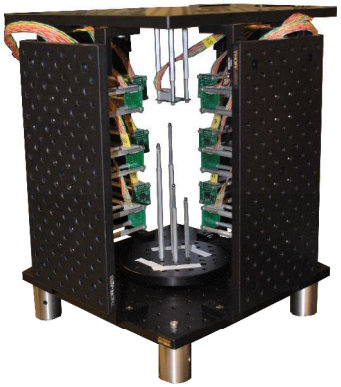

Particle Position and Orientation Tracking

Sensing temperature through stainless steel tube

**Summary**

- Described wireless temperature sensor using permanent magnets
- Created method for measuring the temperature of multiple magnets simultaneously
- Method can track the temperature of moving magnets if calibrated
- Described temperature estimation error analysis methods and experiment design methodology
- Measuring temperatures inside metal vessels or with moving stainless steel components

**Current Work**

- Evaluate larger arrays of magnet temperature
- Optimize magnet position and orientation
- Simultaneous position, orientation and temperature tracking

# Acknowledgements


- The Laboratory Directed Research and Development program
- Randy Schmitt, Ron Allman and Crystal Glen for there assistance with lab space and facilities
- Amanda Dodd, Emily K. Stirrup, Stephen S. Miller, Harriet Li, and Joseph Buttacci for their previous work and assistance with the project

Sandia National Laboratories

# QUESTIONS?

# References


[1] Kovacs, A., Peroulis, D., and Sadeghi, F., 2007. “Early warning wireless telemeter for harsh-environment bearings”. In IEEE Sensors, pp. 946–949.

[2] Gupta, L. A., and Peroulis, D., 2013. “Wireless temperature sensor for condition monitoring of bearings operating through thick metal plates”. IEEE Sensors Journal, 13(6), pp. 2292–2298.

[3] Gupta, L. A., Young, L., Wondimu, B., and Peroulis, D., 2013. “Wireless temperature sensor for mechanical face seals using permanent magnets”. Sensors and Actuators A, 203, pp. 369–372.

[4] Fletcher, R. R., and Gershenfeld, N. A., 2000. “Remotely interrogated temperature sensors based on magnetic materials”. IEEE Transactions on Magnetics, 36(5), pp. 2794– 2795.

[5] Mavrudieva, D., Voyant, J.-Y., Kedous-Lebouc, A., and Yonnet, J.-P., 2008. “Magnetic structures for contactless temperature sensor”. Sensors and Actuators A, 142, pp. 464–467.

[6] Fletcher, R., and Gershenfeld, N., 2001. Wireless monitoring of temperature. US Patent 6,208,253 B1.

[7] Gupta, L. A., and Peroulis, D., 2012. “Wireless temperature sensor operating in complete metallic environment using permanent magnets”. IEEE Transactions on Magnetics, 48(11), pp. 4413–4416.

[8] Yang, W., Hu, C., Li, M., Meng, M. Q.-H., and Song, S., 2010. “A new tracking system for three magnetic objectives”. IEEE Transactions on Magnetics, 46(12), pp. 4023– 4029.

[9] Lee, K.-M., and Son, H., 2007. “Distributed multipole model for design of permanent-magnet-based actuators”. IEEE Transactions on Magnetics, 43(10), pp. 3904–3913.

[10] Wu, F., Frey, D. D., and Foong, S., 2013. “A hybrid magnetic field model for axisymmetric magnets”. In IEEE/ASME International Conference on Advanced Intelligent Mechatronics, pp. 786–791.

[11] Foong, S., Lee, K.-M., and Bai, K., 2012. “Harnessing embedded magnetic field for angular sensing with nanodegree accuracy”. IEEE/ASME Transactions on Mechatronics, 17(4), pp. 687–696.

[12] Hu, C., Meng, M. Q.-H., and Mandal, M., 2006. “The calibrationmof 3-axis magnetic sensor array system for tracking wireless capsule endoscope”. In Proceedings of the 2006 IEEE/RSJ International Conference on Intelligent Robots and Systems, pp. 162–167.

[13] Rynne, B. P., and Youngson, M. A., 2008. Linear Functional Analysis, 2nd ed. London: Springer.

[14] Carpenter Technology Corporation, 2016. Magnetic properties of stainless steels. [Online]. Available: http://www.cartech.com/techarticles.aspx?id=1476

Sandia National Laboratories

# BACKUP SLIDES

# External Disturbances

| Material | $\mu_r$ Ref. [14] | Field Deviation (%) | Repeatability (G) |
|---|---|---|---|
| Air | 1 | $0.06 \pm 0.04$ | $0.10 \pm 0.08$ |
| Copper | 1 | $0.06 \pm 0.05$ | $0.15 \pm 0.09$ |
| Aluminum 6061 | 1 | $0.06 \pm 0.04$ | $0.15 \pm 0.13$ |
| Stainless 304 (Austenitic) | 1 to 7 | $0.50 \pm 0.52$ | $0.14 \pm 0.12$ |
| Stainless 313 (Austenitic) | 1 to 7 | $0.54 \pm 0.37$ | $0.11 \pm 0.09$ |
| Stainless 410 (Martensitic) | 95 to 750 | $34.0 \pm 3.48$ | $0.14 \pm 0.10$ |
| Stainless 430 (Ferritic) | 1800 | $86.6 \pm 4.90$ | $0.16 \pm 0.10$ |

- ~1.3 mm thick metal plates were moved between a magnet and sensor placed 32 mm apart
- The field deviation was measured showing significant changes for materials with relative permeability $\mu_r \neq 1$
- The repeatability of the measurements does not change. Therefore, as long as these high permeability materials are tracked, we can continue to use them during temperature sensing
- The $\mu_r \neq 1$ materials contribute nonlinearly to the field, so calibrations must be done of each combination of the position of the material and magnets.

# 3x3 Experimental Arrangement

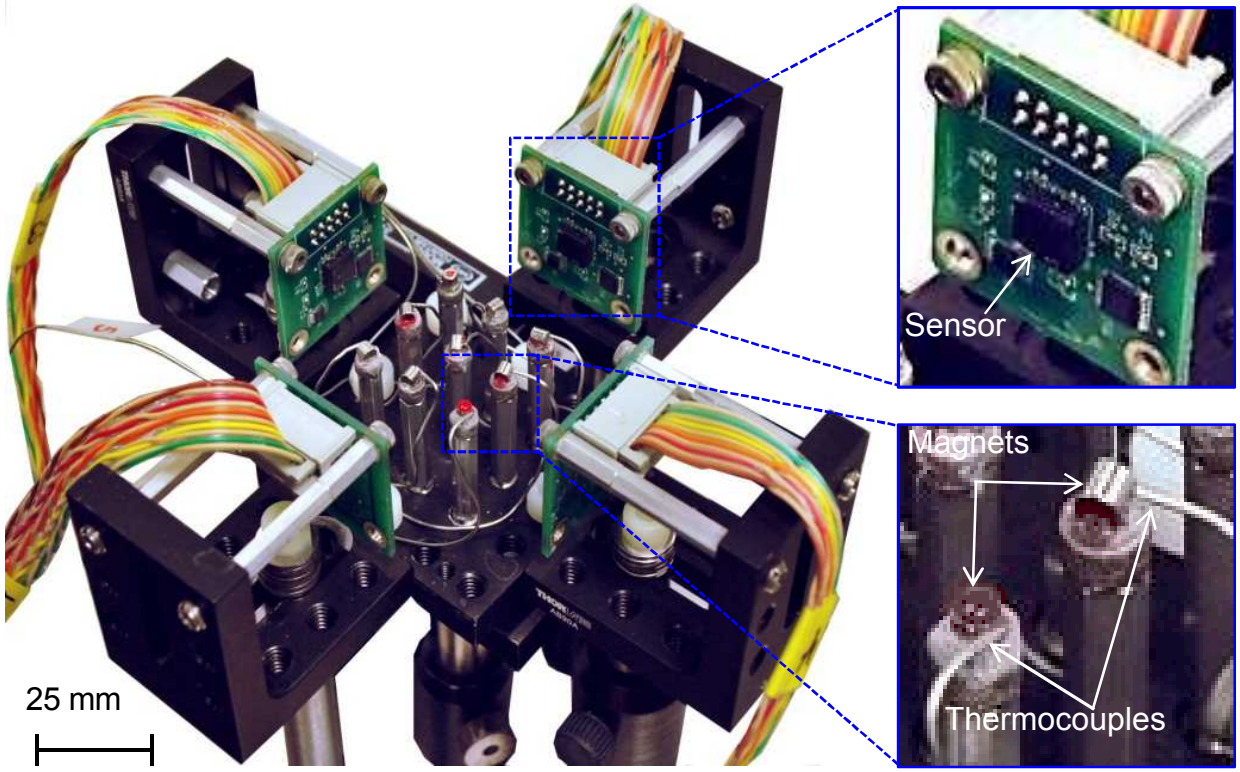

# Matrix Rank and Determinant

Sandia National Laboratories

$rank(\mathbf{P}^T\mathbf{P}) = 3$
Normalized $|det(\mathbf{P}^T\mathbf{P})| = 1.0$

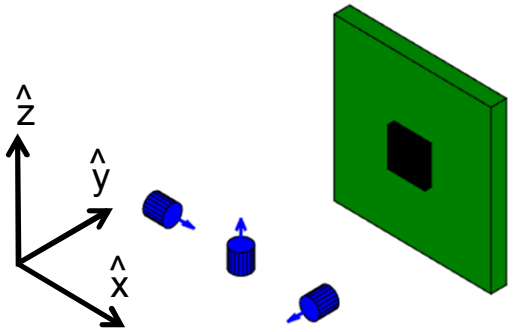


$rank(\mathbf{P}^T\mathbf{P}) = 3$
Normalized $|det(\mathbf{P}^T\mathbf{P})| = 0.51$

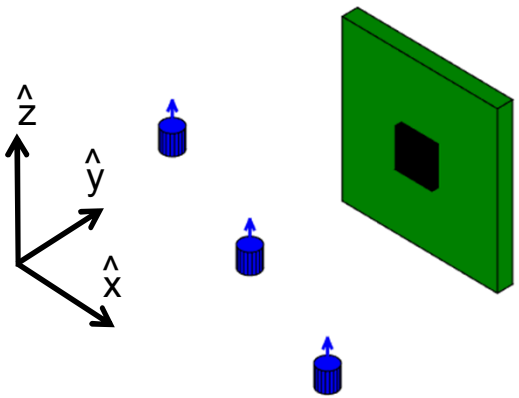


$rank(\mathbf{P}^T\mathbf{P}) = 2$
Normalized $|det(\mathbf{P}^T\mathbf{P})| = 0$

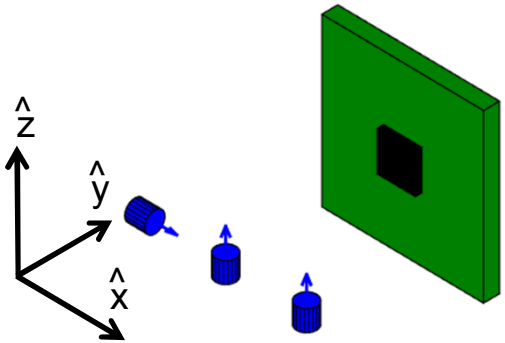


$rank(\mathbf{P}^T\mathbf{P}) = 1$
Normalized $|det(\mathbf{P}^T\mathbf{P})| = 0$

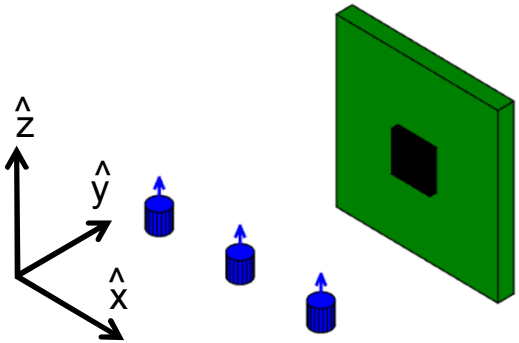

# Magnet Time Constants and Properties

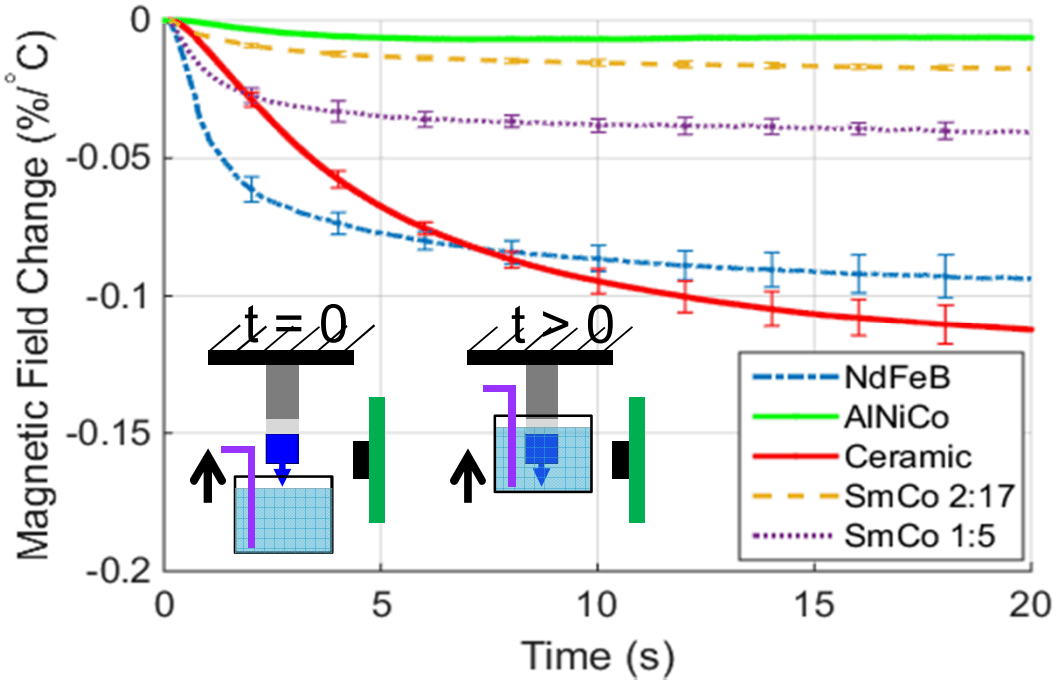


| Type | D (mm) | L (mm) | $P_C$ | Normalized $\bar{B}_z$ (G) *†‡ | $C_T$ (%/°C) * | Measured $\tau$ (s) * | Normalized $\bar{\tau}$ (s) ‡ |
|---|---|---|---|---|---|---|---|
| Nd-Fe-B | 3.175 | 3.175 | 3.24 | 3.43± 0.19 | -0.095 ± 0.014 | 2.29 ± 0.28 | 1.91 ± 0.23 |
| Al-Ni-Co | 3.175 | 3.175 | 3.24 | 1.22± 0.07 | -0.007 ± 0.001 | 2.39 ± 0.34 | 1.99 ± 0.28 |
| Ceramic | 6.35 | 7.137 | 3.99 | 0.71± 0.13 | -0.117 ± 0.011 | 6.17 ± 0.93 | 2.53 ± 0.38 |
| Sm-Co 2:17 | 6.35 | 2.54 | 0.80 | 2.65± 0.04 | -0.017 ± 0.001 | 3.05 ± 0.18 | 1.65 ± 0.10 |
| Sm-Co 1:5 | 3.175 | 3.175 | 3.24 | 2.55± 0.02 | -0.039 ± 0.003 | 1.85 ± 0.34 | 1.54 ± 0.28 |

* Obtained from time constant experiments up to 40°C for Nd-Fe-B and 60°C for other types. Four measurements were taken of each magnet type.
† The magnetic field values were measured from a distance of 19 mm from the magnet center to the sensor center and can be used to compare the field strengths of each magnet type.
‡ For magnet $j$ in each row, the normalization is conducted such that, $\bar{B}_z = B_z V_0/V_j$ and $\bar{\tau} = \tau(A_{sj}V_0)/(A_{s0}V_j)$ where $V_0$ is the volume and $A_{s0}$ is the total surface area of the Nd-Fe-B magnet. Note that $V_j$ is the volume and $A_{sj}$ is the surface area exposed to the fluid for magnet $j$.

# Temperature Constant Calibration

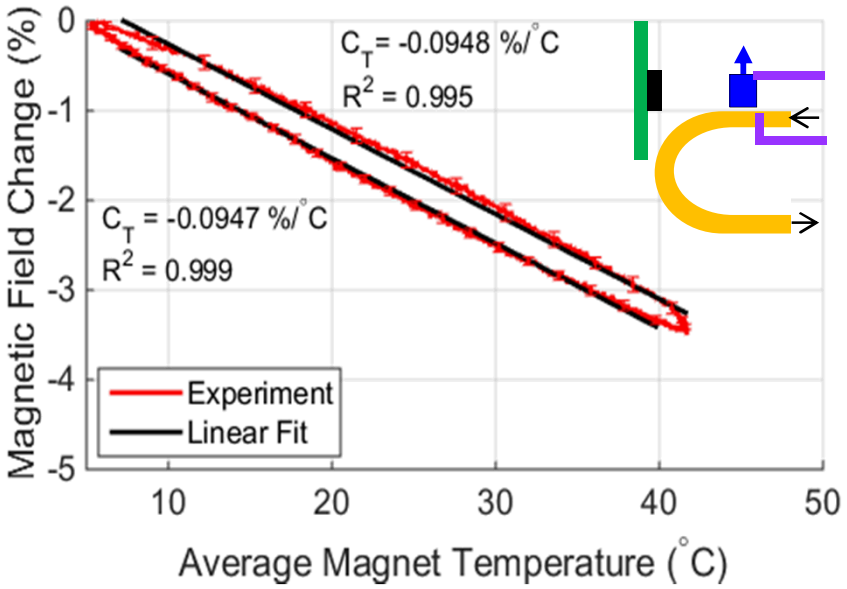


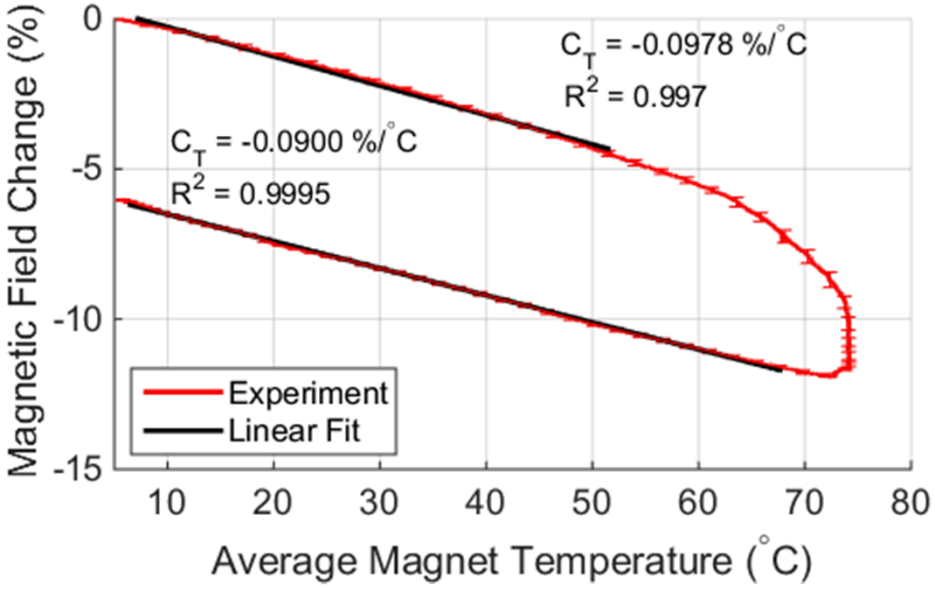

# Non-optimal configuration of 9 magnets

Sandia National Laboratories

Configuration A

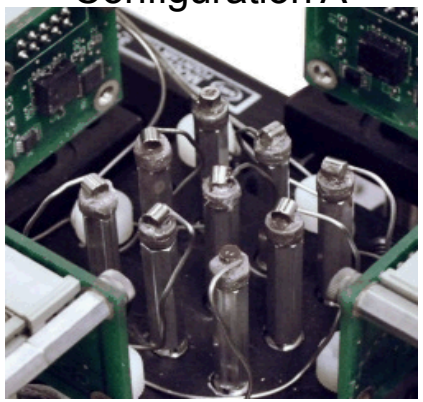

Configuration A

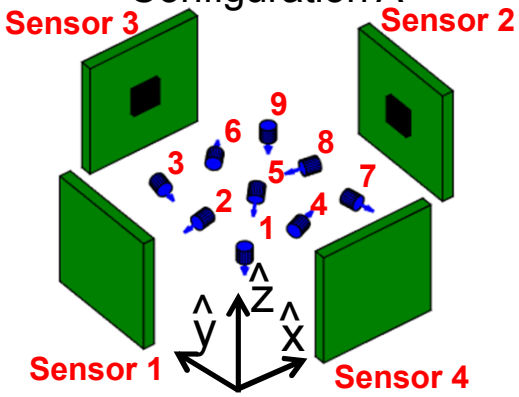


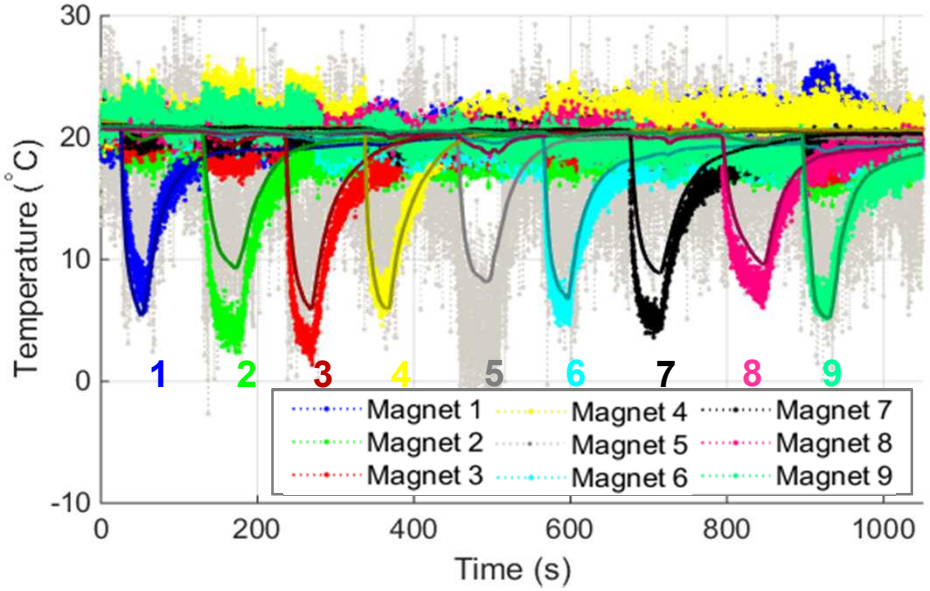

# Optimal configuration of 9 magnets

Sandia National Laboratories

Configuration B

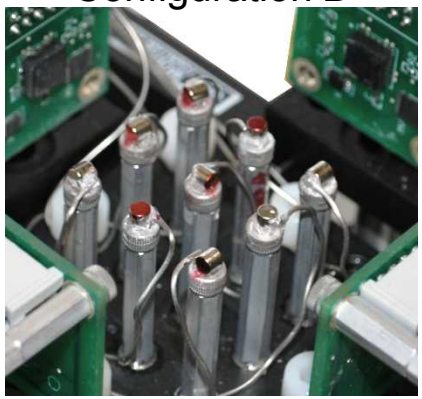

Configuration B

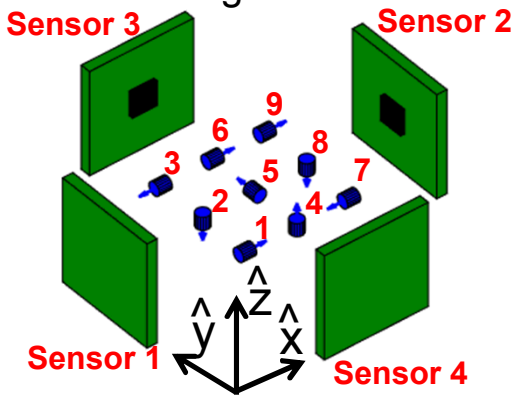


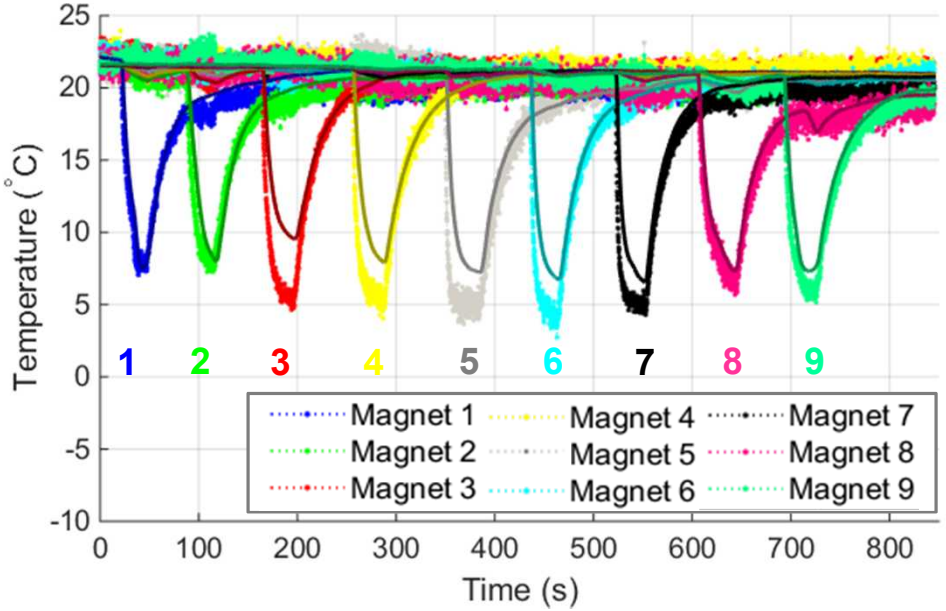

# Temperature Error Metrics

Sandia National Laboratories

EXPERIMENTAL CONDITION NUMBER AND TEMPERATURE ESTIMATE STANDARD DEVIATION AS A FUNCTION OF INVERSION DIMENSIONS

| Setup Configuration | Inversion Dimensions | Condition Number | Experimental Temperature Standard Deviation $\epsilon_T$ | | | | | | | | |
|---|---|---|---|---|---|---|---|---|---|---|---|
| | | | Magnet 1 (°C) | Magnet 2 (°C) | Magnet 3 (°C) | Magnet 4 (°C) | Magnet 5 (°C) | Magnet 6 (°C) | Magnet 7 (°C) | Magnet 8 (°C) | Magnet 9 (°C) |
| A, Fig.8(d) | 9 magnets, 12 axes | 967 | 0.865 | 0.777 | 0.557 | 0.812 | 3.67 | 0.588 | 0.556 | 0.591 | 0.749 |
| A | 9 magnets, 9 axes[1] | $4.19\times10^5$ | 18.8 | 16.5 | 8.75 | 20.4 | 78.4 | 9.29 | 23.1 | 7.24 | 12.6 |
| A | 9 magnets, 9 axes[3] | $1.37\times10^3$ | 0.951 | 0.900 | 0.573 | 0.946 | 4.50 | 0.734 | 0.565 | 0.748 | 0.963 |
| A, Fig.8(e) | 8 magnets[2], 12 axes | 19.9 | 0.448 | 0.332 | 0.401 | 0.289 | N.A. | 0.240 | 0.446 | 0.304 | 0.522 |
| A | 8 magnets[2], 8 axes[4] | 42.9 | 0.687 | 0.322 | 0.385 | 0.300 | N.A. | 0.241 | 0.479 | 0.318 | 0.649 |
| B, Fig.9(c) | 9 magnets, 12 axes | 9.98 | 0.270 | 0.345 | 0.238 | 0.356 | 0.477 | 0.399 | 0.243 | 0.451 | 0.268 |
| B | 9 magnets, 9 axes[1] | $5.76\times10^4$ | 0.972 | 7.25 | 0.304 | 37.5 | 2.07 | 0.414 | 0.822 | 8.54 | 0.546 |
| B | 9 magnets, 9 axes[5] | 56.9 | 0.293 | 0.350 | 0.253 | 0.366 | 1.18 | 0.417 | 0.630 | 0.509 | 0.704 |
| B | 8 magnets[2], 12 axes | 8.82 | 0.271 | 0.343 | 0.240 | 0.355 | N.A. | 0.401 | 0.243 | 0.442 | 0.225 |
| B | 8 magnets[2], 8 axes[6] | 9.47 | 0.381 | 0.350 | 0.238 | 0.370 | N.A. | 0.414 | 0.458 | 0.472 | 0.287 |

The condition number was derived from the $\mathbf{P}^\intercal\mathbf{P}$ matrix and the estimated temperature noise (standard deviation) of each magnet was measured by taking the first 10 s (sampled at 10 Hz) in the data from Fig 8 and Fig 9 when no temperature sources were applied.

[1] For this solution, sensor 4 was dropped from the inversion process.

[2] For this solution, magnet 5 was dropped from the inversion process.

[3] For this solution, sensor 1 axis x, sensor 1 axis z, and sensor 2 axis x were dropped from the inversion process.

[4] For this solution, sensor 1 axis x, sensor 1 axis z, sensor 2 axis x, and sensor 2 axis z were dropped from the inversion process.

[5] For this solution, sensor 2 axis z, sensor 3 axis y, and sensor 4 axis x were dropped from the inversion process.

[6] For this solution, sensor 2 axis z, sensor 3 axis y, sensor 4 axis x, and sensor 4 axis y were dropped from the inversion process.

# Experiments inside metal vessels